Anal. Chem. **2010,** *82,* 10075–10082

Electrochemical Detection of Peroxynitrite Using a Biosensor Based on a Conducting Polymer−Manganese Ion Complex

Wei Choon Alvin Koh,[†] Jung Ik Son,[†] Eun Sang Choe,[‡] and Yoon-Bo Shim*,[†]

Department of Chemistry, Institute of BioPhysio Sensor Technology and Department of Biological Sciences, Pusan National University, Busan 609-735, Korea

A peroxynitrite ($ONOO^-$) biosensor has been developed through the preparation of a new manganese−[poly-2,5-di-(2-thienyl)-1*H*-pyrrole)-1-(*p*-benzoicacid)](Mn−pDPB) complex. DPB monomer was first synthesized and polymerized for the purpose of providing a polymer backbone for complex formation with Mn^{2+} ion. The Mn−pDPB complex was characterized via Magnetomotive Force (MMF) simulation, X-ray photoelectron spectroscopy (XPS), and cyclic voltammetry. The complex selectively enhanced the reduction process of $ONOO^-$ which was used as the analytical signal for chronoamperometric detection. A polyethyleneimmine (PEI) layer was coated on the complex surface to increase selectivity and stability. The chronoamperometric calibration plot showed the hydrodynamic range of 2.0×10^{-8}−5.0×10^{-7} M. The detection limit was determined to be $1.9\ (\pm 0.2) \times 10^{-9}$ M based on S/N = 3. The microbiosensor, fabricated on a 100 μm diameter Pt tip, was applied in a real rat plasma sample for the detection of spiked concentrations of $ONOO^-$. The reliability and long-term stability of the microbiosensor was also examined with YPEN-1 cells in vitro, and the results shown were promising.

Peroxynitrite ($ONOO^-$) is a very powerful oxidant and cytotoxic agent produced in biological systems by the recombination of nitric oxide and superoxide anion radical. $ONOO^-$ has been a source of both exciting discovery and vibrant debate within the broad community of chemically oriented biologists. Because of the reaction rate of its ubiquitous precursors, one can expect to always contend with the direct and secondary reactions of $ONOO^-$. Research in this area has solidly established the contribution of $ONOO^-$ to the fundamental regulation of redox-dependent cell signaling,[1] hemostasis,[2] and host defense.[3] Also, when xenobiotic exposure and inflammatory responses accelerate the generation of superoxide and nitric oxide, $ONOO^-$ further contributes to autoimmune, neurodegenerative, apoptotic, genotoxic, and an abundance of target molecule reactions that affect all aspects of tissue and cellular existence.[4−6] While stabilized as an anion at high pH, $ONOO^-$ has a relatively short half-life (~1 s) under physiological conditions due to rapid reaction with biological targets and molecular decomposition via rearrangement or hemolytic scission.[7] The most useful markers for $ONOO^-$ formation in this context are nitration and hydroxylation products and the dimerization of tyrosine residues.[8]

The use of synthetic $ONOO^-$ in model systems and the rigorous use of controls in biological systems (e.g., $ONOO^-$ scavengers and suppression of superoxide and nitric oxide concentrations) have provided a solid foundation of knowledge that encourages the significance of this species as a dynamic redox signaling mediator and, at higher rates of production, a toxicant.[9] Thus, it is important to quantify the details of $ONOO^-$ production in biological tissues, including direct measurement. For detection of $ONOO^-$, a variety of sensor systems has been developed. Mass spectrometric and immunodetection of nitrotyrosine is typically applied for the presence of biological $ONOO^-$ formation.[8,10] Other methods have also been developed for the detection of $ONOO^-$, such as UV−visible spectroscopy, electron spin resonance spectroscopy, chemiluminescence, and fluorescence.[11−15] These analytical techniques allow the specific determination of $ONOO^-$, but they are complicated, time-consuming, and require costly equipment. Otherwise, electrochemical methods are most advantageous because of their simplicity, speed, and sensitivity as well as being able to perform measurements due to miniaturization of sensor elements.[16] Disadvantages of electrochemical methods include fouling of the biosensor surface and low selectivity. To

* Corresponding author. Phone:(+82) 51 510 2244. Fax: (+82) 51 514 2430. E-mail: ybshim@pusan.ac.kr.

[†] Department of Chemistry, Institute of BioPhysio Sensor Technology.

[‡] Department of Biological Sciences.

(1) Tarpey, M. M.; Fridovich, I. *Circ. Res.* **2001**, *89*, 224–236.
(2) Eaton, P.; Clements-Jewery, H. *Br. J. Pharmacol.* **2008**, *155*, 972–973.
(3) Habib, S.; Moinuddin; Ali, A.; Ali, R. *Cell. Immunol.* **2009**, *254*, 117–123.
(4) Woodcock, S. R.; Freeman, B. A. *Chem. Res. Toxicol.* **2008**, *21*, 2227–2228.
(5) Starodubtseva, M. N.; Tattersall, A. L.; Kuznetsova, T. G.; Yegorenkov, N. I.; Ellory, J. C. *Biochemistry* **2008**, *73*, 155–162.
(6) Arbault, S.; Sojic, N.; Bruce, D.; Amatore, C.; Sarasin, A.; Vuillaume, M. *Carcinogenesis* **2004**, *25*, 509–515.
(7) Beckman, J. S.; Koppenolm, W. H. *Am. J. Physiol.* **1996**, *271*, 1424–1437.
(8) Kirsch, C.; de Groot, H. *J. Biol. Chem.* **2002**, *277*, 13379–13388.
(9) Virag, L.; Szabo, E.; Gergely, P.; Szabo, C. *Toxicol. Lett.* **2003**, *140*, 113–124.
(10) Latal, P.; Kissner, R.; Bohle, D. S.; Koppenol, W. H. *Inorg. Chem.* **2004**, *43*, 6519–6521.
(11) Malinski, T.; Taha, Z. *Nature* **1992**, *358* (6388), 676–678.
(12) Kulagina, N. V.; Zigmond, M. J.; Michael, A. C. *Neuroscience* **2001**, *102*, 121–128.
(13) Boon, E. M.; Marletta, M. A. *J. Am. Chem. Soc.* **2006**, *128*, 10022–10023.
(14) Fabre, B.; Burlet, S.; Cespuglio, R.; Bidan, G. *J. Electroanal. Chem.* **1997**, *426*, 75–83.
(15) Lee, Y. T.; Shim, Y. B. *Anal. Chem.* **2001**, *73*, 5629–5632.

10.1021/ac102041u
Published on Web 11/19/2010

overcome the shortage of these methods, we synthesized a new polymer−Mn^{2+} complex to improve selectivity and examined the reliability of the sensor in $ONOO^-$ detection. The Mn^{2+} ion can enhance the electron transfer reaction involved in the degradation of $ONOO^-$ to nitrogen dioxide and nitrate.[17−19] Thus, we tried to utilize this reaction for the detection of $ONOO^-$.

Conducting polymers, having carboxylic acid as a functional group, can coordinate with a metal ion to form a coordination complex. Electropolymerization provides one of the in situ sensor preparation methods, examples of sensory material being conducting polymers such as polypyrrole[14] and polyterthiophene.[15] These films can be prepared reproducibly and quite thinly, ensuring a rapid and stable response of the sensor.[20,21] The organic functional groups, such as amine, imine, and carboxylic acid can be used as ligands for the metal ion complexation.[22,23] So far, there are few reports of the metal ion complex with conducting polymers due to the weak interaction of conducting polymers with metal ions.[24]

In the present study, in order to more flexibly control the orientation of the carboxylic acid groups outward from the probe surface, we have synthesized a new ligand, 2,5-di-(2-thienyl)-1*H*-pyrrole derivative, [(2,5-di-(2-thienyl)-1*H*-pyrrole)-1-(*p*-benzoic acid)] (DPB). We also studied the preparation and characterization of the Mn−conducting polymer complex (Mn−pDTB)-coated microelectrode and its electrocatalytic activity toward $ONOO^-$ reduction. A polyethyleneimmine (PEI) layer was coated onto the modified electrode surface to increase $ONOO^-$ selectivity and biosensor stability. The experimental parameters such as pH and applied potential were optimized. We demonstrated the biosensor's applicability to the in vitro determination of $ONOO^-$ in a real plasma sample. In addition, the $ONOO^-$ biosensor was also applied to stimulated cultured cells, and the validity of the sensor was evaluated.

EXPERIMENTAL SECTION

Materials. A *ter*-heteroaromatic (thiophene−pyrrole−thiophene) functionalized monomer, 2,5-di(2-thienyl)-1*H*-pyrrole-1-(*p*-benzoic acid) (DPB) was newly synthesized through the Paal−Knorr pyrrole condensation reaction.[25] 1-Ethyl-3-(3-dimethylaminopropyl) carbodiimide (EDC), polyethyleneimmine (PEI), dichloromethane (CH_2Cl_2; 99.8%, anhydrous, sealed under nitrogen gas), hydrogen peroxide (30% solution), manganese sulfate, and cocaine hydrochloride were purchased from Sigma Aldrich (USA). Tetrabutylammonium perchlorate (TBAP, electrochemical grade) was received from Fluka (USA), purified, and then dried under vacuum at 1.33×10^3 Pa. Disodium hydrogen phosphate, sodium dihydrogen phosphate, sodium chloride, sulfuric acid, and ethanol were purchased from Aldrich Chemical Co. (USA). A phosphate buffer saline solution (PBS) was prepared by modifying 0.1 M of disodium hydrogen phosphate and 0.1 M of sodium dihydrogen phosphate with 0.1% sodium chloride. All other chemicals were of extra pure analytical grade and used without further purification. All aqueous solutions were prepared in doubly distilled water, which was obtained from a Milli-Q water purifying system (18 MΩ cm).

Preparation of Peroxynitrite Standard Solutions. $ONOO^-$ was biomimetically synthesized from nitric oxide (NO)[26] and potassium superoxide[27] solutions. $ONOO^-$ was also introduced via a 0.1 mM donor solution of 3-morpholinosydnonimine (SIN-1).[28] The $ONOO^-$ stock solution was stored at −20 °C, and the concentration was verified by UV−visible spectrometry at 302 nm ($\varepsilon = 1670\ mol^{-1}\ L\ cm^{-1}$) just before the experiments.[29]

Microelectrode Preparation. The Pt microelectrode was fabricated and subsequently cleaned by cycling the applied potential between +1.4 and −0.2 V for ten cycles at a scan rate of 500 mV/s in a 0.5 M H_2SO_4 solution followed by washing with distilled water. It was then used in all subsequent experiments according to our previous report.[30]

Peroxynitrite Sensor Fabrication. The Mn−pDPB complexing solution was composed of 1.0 mM Mn^{2+} and 1.0 mM DPB monomer together in a 0.1 M TBAP/CH_2Cl_2 solution. Electropolymerization on the microelectrode surface was performed by cycling the potential between 0 and 1.4 V two times at the scan rate of 100 mV/s. After that, the electrode was washed with CH_2Cl_2 to remove the excess monomer. Gold nanoparticles (AuNPs) were then electrodeposited on the modified electrode surface using linear sweep voltammetry. PEI coating was performed by dipping the Mn−pDPB complex-modified electrode three times in a 1% PEI solution. The modified electrode was completely dried after PEI coating.

Instruments. A Mn−pDPB complex-modified microelectrode, Ag/AgCl (in saturated KCl), and a Pt wire were used as working, reference, and counter electrodes, respectively. Cyclic voltammograms and chronoamperograms were recorded using a potentiostat/galvanostat, Kosentech Model KST-P2 (South Korea). Electron spectroscopy for chemical analysis (ESCA) experiments were done using a VG Scientific ESCALAB 250 XPS spectrometer with a monochromated Al Kα source and charge compensation (Korea Basic Science Institute, Busan). ChemDraw Ultra and MM2 software were used for 3D structure stimulation and binding energy calculation as shown in Figure 1c.

Electrochemical Measurements. Cyclic voltammograms were recorded for the Mn−pDPB microelectrode from −0.2 to 0.6 V versus Ag/AgCl in 0.1 M PBS at pH 7.4. Chronoamperometric experiments were performed by applying the potential of 0.2 V at the Mn−pDPB microelectrode to reduce $ONOO^-$. A

(16) Yang, D.; Wang, H.-L.; Sun, Z.-N.; Chung, N.-W.; Shen, J.-G. *J. Am. Chem. Soc.* **2006**, *128*, 6004–6005.
(17) Xue, J.; Ying, X.; Chen, J.; Xian, Y.; Jin, L. *Anal. Chem.* **2000**, *72*, 5313–5321.
(18) Cortes, J. S.; Granados, S. G.; Ordaz, A. A.; Jimenez, J. A. L.; Griveau, S.; Bedioui, F. *Electroanalysis* **2007**, *1*, 61–64.
(19) Viggiano, A. A.; Midey, A. J.; Ehlerding, A. *Int. J. Mass Spectrom.* **2006**, *255*, 65–70.
(20) Rahman, M. A.; Kwon, N.-H.; Won, M. S.; Choe, E. S.; Shim, Y.-B. *Anal. Chem.* **2005**, *77*, 4854–4860.
(21) Rahman, M. A.; Park, D.-S.; Chang, S. C.; McNeil, C. J.; Shim, Y.-B. *Biosens. Bioelectron.* **2006**, *21*, 1116–1124.
(22) Cotton, F. A.; Wilkinson, G. *Advanced Inorganic Chemistry*; John Wiley & Sons: New York, 1988.
(23) Mehrotra, R. C.; Bohra, R. *Metal Carboxylates*; Academic Press: London, 1983.
(24) Rahman, M. A.; Lee, K.-S.; Park, D.-S.; Won, M.-S.; Shim, Y.-B. *Biosens. Bioelectron.* **2008**, *23*, 857–864.
(25) Amarnath, V.; Anthony, D. C.; Amarnath, K.; Valentine, W. M.; Wetterau, L. A.; Graham, D. G. *J. Org. Chem.* **1991**, *56*, 6924–6931.
(26) Pallini, M.; Curulli, A.; Amine, A.; Palleschi, G. *Electroanalysis* **1998**, *10*, 1010–1016.
(27) Ge, B.; Lisdat, F. *Anal. Chim. Acta* **2002**, *454*, 53–64.
(28) Ashki, N.; Hayes, K. C.; Bao, F. *Neuroscience* **2008**, *156*, 107–117.
(29) Vander, V. A.; Eiserich, J. P.; O'Neill, C. A. *Arch. Biochem. Biophys.* **1995**, *319*, 341–349.
(30) Koh, W. C. A.; Rahman, M. A.; Choe, E. S.; Lee, D. K.; Shim, Y.-B. *Biosens. Bioelectron.* **2008**, *23*, 1374–1381.

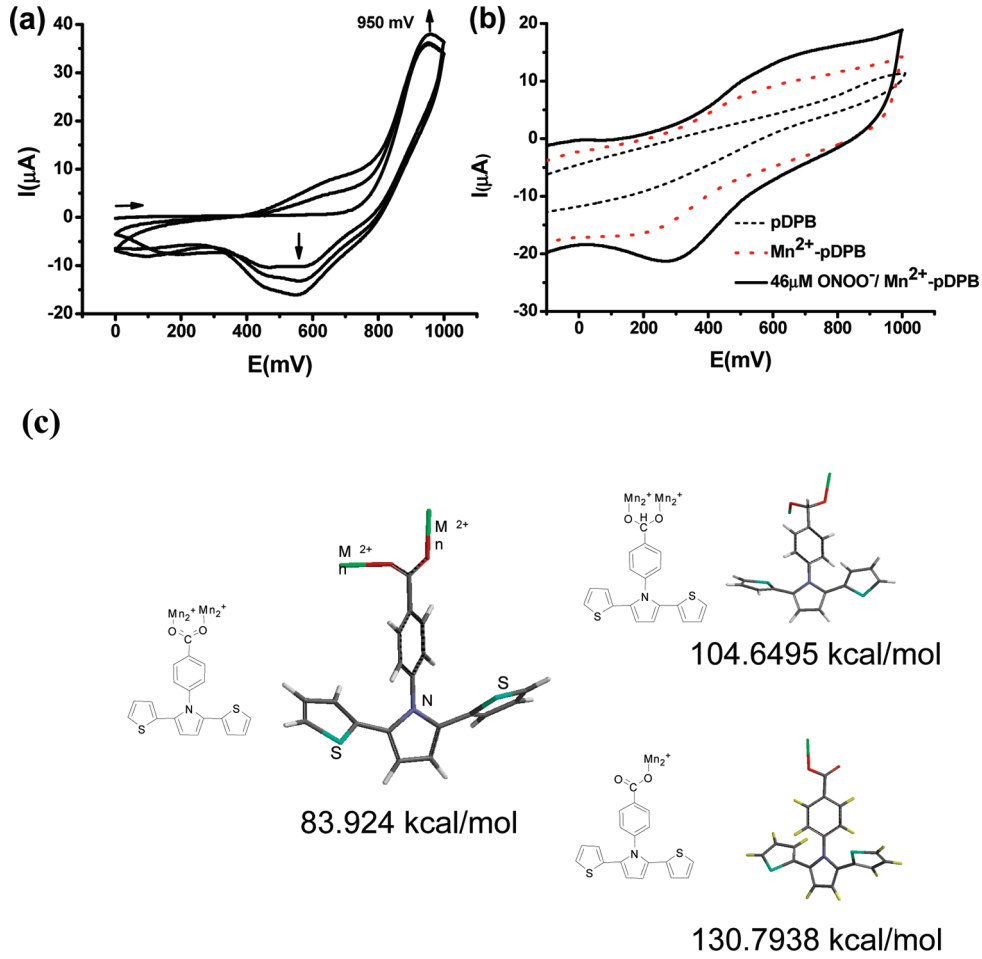

Figure 1. (a) Cyclic voltammograms recorded for the electropolymerization of DPB monomer in a 0.1 M TBAP/CH_2Cl_2 for three consecutive potential cycles. (b) CVs of the Mn−pDPB complex-modified surface without peroxynitrite (0 μM), in the presence of peroxynitrite (46 μM), and only on the pDPB surface. (c) 3D image stimulation and calculated MMF energies of Mn−pDPB structure.

freshly prepared 4.0 mL aliquot of 0.1 M PBS was added into the electrochemical cell, and the steady-state current was monitored with the Mn−pDPB microelectrode at the optimal pH and temperature. Consecutive injections of varying amounts of $ONOO^-$ into the cell and their amperometric responses were monitored. In in vitro experiments, there was a three-electrode configuration where the $ONOO^-$ microbiosensor, Ag/AgCl electrode, and Pt wire were used as the working, reference, and counter electrodes, respectively. All biosensors were calibrated at 25 ± 1 °C.

Blood Plasma Sample. The rat blood plasma real sample was prepared according to the following procedure; at first, 2 μg/mL heparin was added to the rat blood samples to prevent coagulation. The blood plasma was then centrifuged for 15 min at 4000 rpm. The liquid was then centrifuged twice at 10 000 rpm for 15 min each time before the experiments.

Cell Culture Sample. YPEN-1 glioma cells (American Type Culture Collection, anassas, VA) were cultured in Dulbecco's Modified Eagle's Medium (Gibco), supplemented with 15% fetal calf serum (Gibco), 0.1 mM mercaptoethanol (Sigma), 0.1 mM nonessential amino acids (Gibco), 100 U/mL penicillin, and 100 mg/mL streptomycin (Gibco). Briefly, cells were trypsinized and suspended in 10 mL of differentiation medium (Iscove's Modified Dulbecco's Media), 15% FBS, 2.0 mM L-glutamine, 0.1 mM nonessential amino acids, 100 U/mL penicillin, and 100 mg/mL streptomycin and cultured in 100 mm nonadhesive Petri dishes to allow cells to aggregate and form embryoid bodies (EBs). The medium was replaced every 2 days. Cells were plated on 0.1% gelatin coated Petri dishes.

RESULTS AND DISCUSSION

Preparation and Characterization of the Mn−pDPB Microelectrode. The schematic representation of the preparation of the Mn−pDPB complex on the electrode is shown in Scheme 1. The nanoparticle comprised conducting polymer layer onto a microelectrode was obtained through the electropolymerization reaction of 1.0 mM DPB monomer containing 1.0 mM Mn^{2+} in a 0.1 M TBAP/CH_2Cl_2 solution by cycling the potential between 0 and 1.4 V two times at the scan rate of 100 mV/s. As shown in Figure 1a, an increasing reduction and oxidation peak for DPB with each potential cycle was obtained at 570 and 950 mV, respectively, after the oxidation of monomer at +900 mV. Redox peaks for Mn^{2+} ion were not clearly shown because DPB has redox peaks of a much higher magnitude than Mn^{2+} due to the relatively low electroactivity of Mn^{2+} in nonaqueous

Scheme 1. Fabrication Steps of Mn−pDPB Modified Electrode and Reaction Mechanism Scheme of the Mn−pDTB Modified Electrode with ONOO⁻

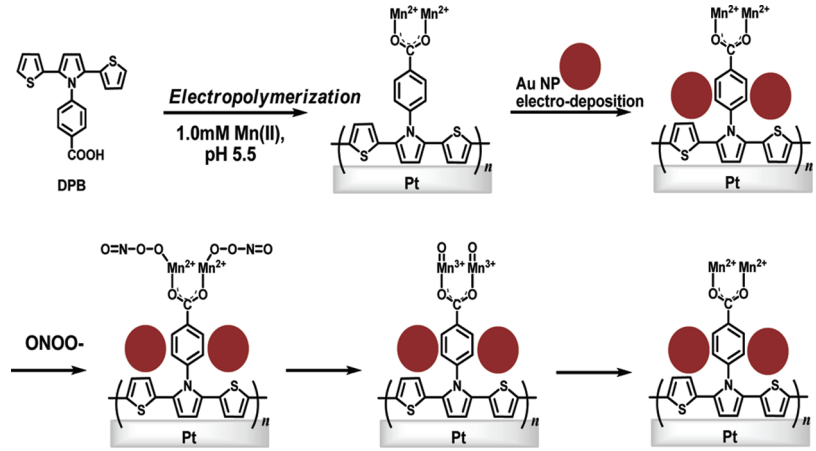

solution.[31] After that, the electrode was washed with CH_2Cl_2 to remove the excess monomer. Gold nanoparticles (AuNPs) were then electrodeposited on the modified electrode surface. The Mn−pDPB modified electrode was coated with a film of PEI. The modified electrode was completely dried after PEI coating. Figure 1b shows the CVs recorded for a Mn−pDPB complex-modified electrode (dotted line) in a phosphate buffer solution (PBS) of pH 7.4. A redox peak was clearly observed at +550/+200 mV vs Ag/AgCl. The redox peak was not observed when the CV was recorded for a mere pDPB-coated electrode as shown in Figure 1b (dashed line). This indicates that the redox peak originated from the Mn species complexed with pDPB. The anodic peak at +550 mV corresponded to the oxidation of Mn^{2+} to Mn^{3+}, whereas the cathodic one at +200 mV corresponded to the reduction of Mn^{3+} to Mn^{2+}. It was previously reported for a MnO_2 film-modified CPE system used to study Mn oxidation states which showed a reduction signal at +300 mV.[32] In this case, the signal was attributed to formation of lower oxidation state manganese oxides. Above 400 mV, reoxidation of these oxides to MnO_2 occurred. The oxides (+400 mV) showed a similar oxidation potential to ours (+550 mV), but the reduction potential of our system (+200 mV) was different from the oxide system. This indicates that the oxidation of Mn^{2+} to Mn^{3+} is similar, but the reduction of oxidized Mn species is a little different due to the different coordination environment in our Mn−pDPB complex system. When $ONOO^-$ (46 μM) was added in a 0.1 M phosphate buffer solution at pH 7.4, there was a slight positive shift in the reduction peak, showing the interaction of Mn attached on the pDPB (Figure 1b, bold line). The three possible 3-dimensional structures of Mn−pDPB were emulated by ChemDraw Ultra in simulation, and their stabilized molecular energies were calculated using Magnetomotive Force (MMF) as shown in Figure 1c. The most stable molecule was shown to have molecular binding energy of 83.924 kcal/mol corresponding to C sharing a double bond with 2 O atoms, each subsequently linked to Mn^{2+} ion.

The cathodic and anodic peak currents were dependent on the scan rate (data not shown). The electron transfer rate constant, k_s, for this process was determined to be 2.73 s^{-1} with the Laviron equation,[33] which shows a 5-fold enhancement in the $ONOO^-$ reduction process due to the presence of Mn^{2+} ion involved in electron transfer compared to the previous reports.[18,19] The maximum surface coverage of the complexed Mn^{2+} on the pDPB film at the optimized condition was estimated using the following equation:[34]

$$I_P = n^2F^2\nu A\Gamma/4RT$$

where I_p is the peak current, n is the number of electrons, F is the Faraday constant, R is the gas constant, T is temperature, ν is the scan rate, A is the area of the electrode, and Γ is the surface coverage of Mn^{2+} species. The surface coverage of the complexed Mn^{2+} species was estimated to be $(5.01 \pm 0.13) \times 10^{-11}$ mol/cm^2 from the oxidation process of Mn^{2+} to Mn^{3+}.

ESCA Characterization of the Mn−pDPB Complex. To characterize the modified surfaces, ESCA analyses were carried out as shown in Figure 2. Figure 2a shows the survey spectra obtained for pDPB (dashed line) and Mn−pDPB complex-modified surfaces (solid line). The pDPB-coated surface did not show any peak for Mn, whereas the Mn−pDPB complex-modified surface showed two Mn2p peaks, indicating that the Mn^{2+} species was present in the Mn−pDPB complex-modified surface.[35] The O1s spectrum shown in Figure 2b for the pDPB-coated surface exhibited a peak at 532.0 eV (dashed line), which corresponded to the C−O bond. The peak shifted to a higher energy of 532.6 eV (solid line) after complexation. This indicated that the complex formation between Mn^{2+} and pDPB occurred through the formation of Mn^{2+}−O bonds. The ESCA spectra of Mn2p peaks in Figure 2c for the Mn−pDPB complex-coated surface were recorded before any redox potential was applied to the electrode. The Mn2p spectrum exhibited two peaks at 641.2 and 652.9 eV which corresponded to $2p_{3/2}$ and $2p_{1/2}$ environments, respectively. To identify the oxidation states of Mn species during the redox reaction, ESCA spectra were taken for the Mn−pDPB

(31) Sarneski, J. E.; Brzezinski, L. J.; Anderson, B.; Didiuk, M.; Manchanda, R.; Crabtree, R. H.; Brudvig, G. W.; Schulte, G. K. *Inorg. Chem.* **1993**, *32*, 3265–3269.
(32) Beyene, N. W.; Kotzian, P.; Schachl, K.; Alemu, H.; Turkusic, E.; Copra, A.; Moderegger, H.; Svancara, I.; Vytras, K.; Kalcher, K. *Talanta* **2004**, *64*, 1151–1159.
(33) Laviron, E. *J. Electroanal. Chem.* **1979**, *101*, 19–28.
(34) Bard, A. J.; Faulkner, L. R. *Electrochemical Methods*; Wiley: New York, 1980.
(35) Zaw, M.; Chiswell, B. *Talanta* **1995**, *42*, 27–40.

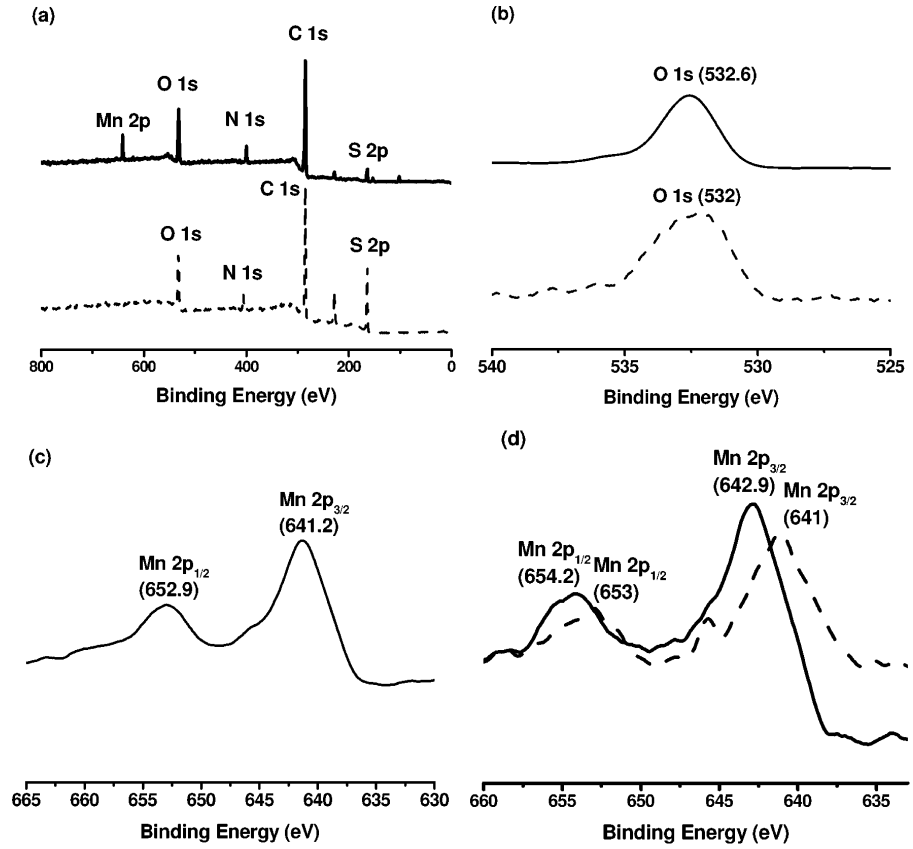

Figure 2. ESCA analysis of pDPB-coated (dashed line) and Mn−pDPB complex-modified (solid line) surfaces; (a) survey spectra, (b) O1s peaks before (dashed line) and after (solid line) complexation with Mn^{2+}, (c) Mn2p peaks before application of any potential, and (d) Mn2p peaks of the Mn−pDPB complex-modified surface after oxidation at +550 mV (solid line), oxidized Mn−pDPB complex surface after reduction at +200 mV (dashed line).

complex-modified surface after oxidation at +550 mV and for the oxidized Mn−pDPB complex modified surface after reduction at +200 mV. As shown in Figure 2d, the Mn $2p_{3/2}$ peaks after oxidation, belonging to the Mn^{3+}−pDPB complex modified surface, appeared at 642.9 and 641 eV, which corresponded to the Mn^{3+} and Mn^{2+} species, respectively. After reduction, the Mn $2p_{1/2}$ peaks appeared at 654.2 and 653 eV, corresponding to the Mn^{3+} and Mn^{2+} species, respectively.[35] This clearly showed that Mn^{2+} was first oxidized to Mn^{3+} and then reduced back to Mn^{2+} after reacting with $ONOO^-$. Thus, the redox Mn^{2+}/Mn^{3+} couple chemically adsorbed on pDPB was involved in the $ONOO^-$ detection process.

Optimization of Analysis Parameters. To optimize the sensing condition of the $ONOO^-$ microbiosensor, the pH effect of the medium and the applied reduction potential were studied on the basis of the electrochemical reduction of $ONOO^-$ with the Mn−pDPB modified electrode. The pH effect on analytical sensitivity was studied in the pH range of 4.0−9.0. The response current increased as media pH increased from 4.0 to 7.0 and then showed a decrease above pH 7.5 (Figure 3a). However, the current response did not decrease significantly between pH 7.0 and 7.5. Since the physiological pH in the brain is considered to be 7.4, the calibration experiments were done at pH 7.4.

The temperature dependency tests were carried out using the Mn−pDPB modified electrode at temperatures of 20−60 °C, as shown in Figure 3b. The biosensor response decreased as the temperature increased over 25−60 °C. Hence, all subsequent experiments were performed at the optimal temperature of 25 °C.

The effect of the applied reduction potential on the chronoamperometric response was also studied for the electroreduction of $ONOO^-$ with the Mn−pDPB modified electrode. The current response increased as the applied potential went from 0.6 V to less positive potentials up to 0.2 V, where the maximum response was observed. This tied in well with the cyclic voltammetric results in that the $ONOO^-$ showed a reduction peak at the same value of 0.2 V. The application of more negative potentials up to −0.2 V showed declining current response (Figure 3c). Therefore, the Mn−pDPB modified electrode was polarized at 0.2 V versus Ag/AgCl in the chronoamperometric experiments.

Interference Effect and Selectivity. Oxygen, peroxide, or superoxide species interfere with $ONOO^-$ detection due to their similar molecular size and the fact that they are precursors or byproducts of interlinked biological processes.[1] Thus, there is a need to eliminate these interfering species. Of the ion permeable polymers, PEI does not allow cations to permeate through. In addition, the PEI layer also prevents microelectrode fouling due to nonspecific adsorption of proteins and other biological materials present in the brain.[20] In order to remove interference from positively charged species and ensure long-time stability, a thin PEI film was coated onto the Mn−pDPB

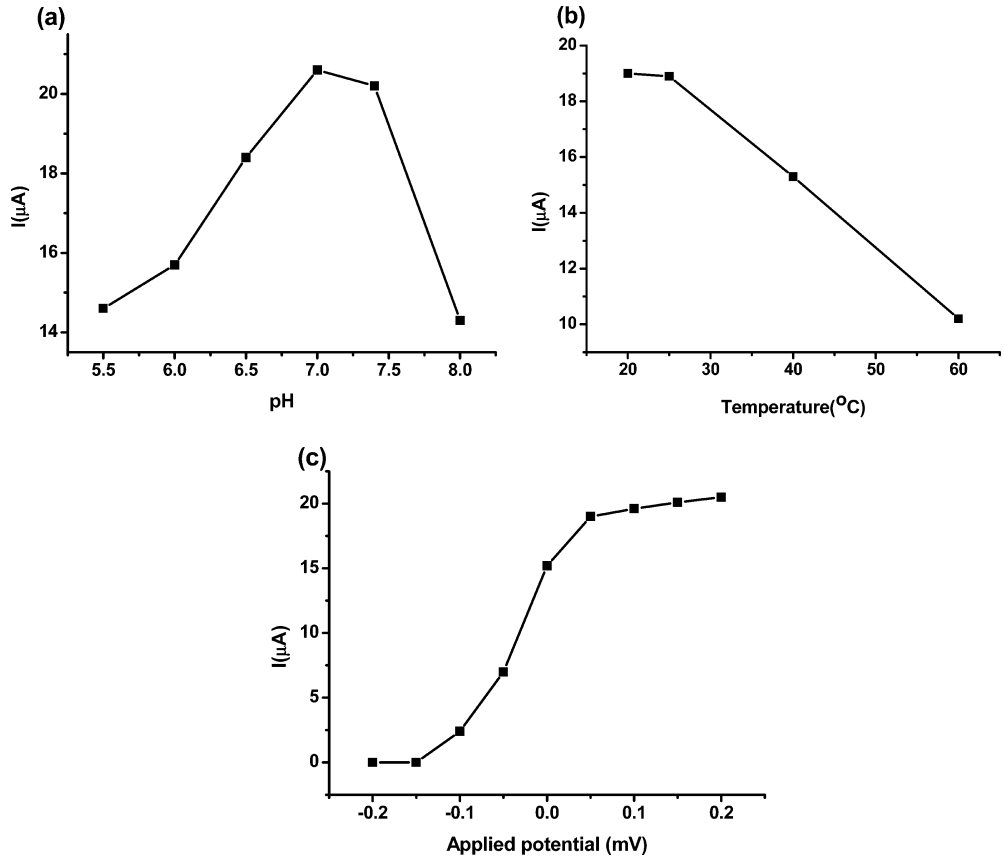

Figure 3. Optimizations of experimental conditions of the $OONO^-$ biosensor; (a) pH, (b) temperature, and (c) applied potential.

surface of the electrode. The selectivity of the Mn−pDPB modified electrode was evaluated with chronoamperometry in the presence of oxygen and other reactive oxygen species, such as hydrogen peroxide and superoxide as shown in Figure 4a. Figure 4a showed a small response to oxygen in the chronoamperogram where oxygen was present in the PBS solution (when no purging was performed with nitrogen). There was little interference when varying amounts of other compounds such as hydrogen peroxide and superoxide were added to the PBS test solution as shown in Figure 4a. $ONOO^-$ was added in the solution in increasing amounts (23, 64, and 140 nM), and the current response of the PEI-coated Mn−pDPB modified electrode increased gradually, indicating that the modified electrode can detect $ONOO^-$ more effectively than other species. To further confirm the response of $ONOO^-$, inhibitory experiments were performed using a chronoamperometric technique where a $ONOO^-$ scavenger, such as uric acid,[1] was added after four successive additions of $ONOO^-$ standard solution (data not shown). The response current rose steeply and then arrived at an increased steady value after each addition of $ONOO^-$. However, upon adding uric acid, the current response declined sharply to the baseline value. This is because $ONOO^-$ was removed from the test solution almost immediately by uric acid.

Calibration Plot. To calibrate the $ONOO^-$ microbiosensor for in vitro measurements, the chronoamperometric response of the Mn−pDPB modified electrode was monitored by introducing varying concentrations of $ONOO^-$ standard solutions. Figure 4b (Inset) showed the typical current−time plots for the addition of various $ONOO^-$ concentrations in a 0.1 M

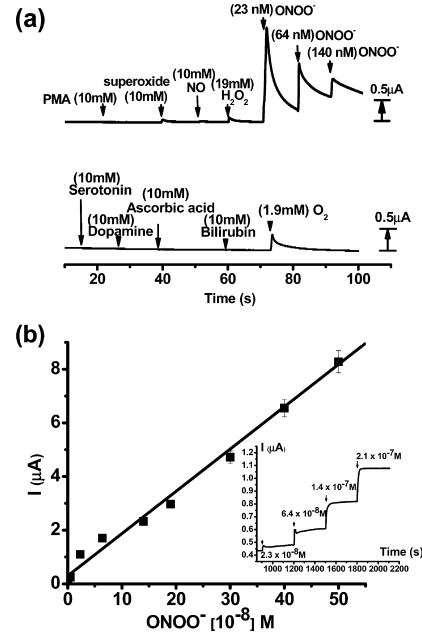

Figure 4. (a) Chronoamperomeric measurements for the interference effects of different compounds with Mn−pDPB complex-modified electrode. (b, inset) Amperometric responses for $ONOO^-$ recorded with Mn−pDPB complex-modified microbiosensor. Applied potential was set at 0.2 V versus Ag/AgCl. (b) Calibration plot for $ONOO^-$ recorded with a Mn−pDPB complex-modified microbiosensor.

PBS solution during experiments. The applied potential was set at 0.2 V for the electroreduction of $ONOO^-$ by the Mn−pDPB modified electrode. The response current rose steeply and then arrived at an increased steady value after each addition of $ONOO^-$. Ninety-five percent of steady-state currents were achieved by the Mn−pDPB modified electrode after about 15 s. Figure 4b showed the calibration plots of the Mn−pDPB modified electrode obtained during an experiment. Under optimized conditions, the steady-state currents exhibited a linear relationship with the $ONOO^-$ concentration in the range of 2.0×10^{-8}–5.0×10^{-7} M for experiments. This range is two orders of magnitude lower than the values in previously reported electrochemical methods which employed the tetraaminophthalocyanine complex film as a sensing element.[17,36] The electrode was found to be reusable eight times, and the relative standard deviation was found to be 3.4%, after five experimental runs. The linear dependencies of $ONOO^-$ concentration gave an equation of i_p (μA) = (0.298 ± 0.16) + (0.157 ± 0.007) [C] (μM), with a correlation coefficient of 0.994. The sensitivity of the $ONOO^-$ microbiosensor was 0.157 ± 0.007 μA/μM. The stability of the $ONOO^-$ microbiosensor was examined using five experimental runs, and the sensitivity of the $ONOO^-$ microbiosensor was maintained at 86% after two months, indicating high sensor stability. The detection limit of $ONOO^-$ was determined to be 1.9 (±0.2) $\times 10^{-9}$ M by the Mn−pDPB modified electrode based on a five times measurement for the standard deviation of the blank noise (95% confidence level, k = 3, n = 5). This was two orders of magnitude lower than previously reported in in vitro $ONOO^-$ sensing.[37,38] Thus, the highly sensitive $ONOO^-$ microsensor was obtained and used in experiments.

Response of the $ONOO^-$ Microbiosensor in Blood Plasma. To examine the validity of the proposed biosensor for the real sample applications, the determination of $ONOO^-$ released in rat blood plasma was studied. Healthy plasma sample does not contain $ONOO^-$, so we performed spike and recovery experiments to examine the applicability of this $ONOO^-$ sensor in a rat plasma sample. The calibration method was used to determine $ONOO^-$ concentration. Figure 5a shows the amperogram recorded during the addition of a 1.0 mL of blood plasma sample, followed by adding different concentrations of a standard solution of $ONOO^-$. The inset of the figure shows the corresponding standard addition plot. The linear regression equation was expressed as I_p (μA) = 1.57 (±0.02) + 0.16 (±0.04) [$ONOO^-$] (μM), with the correlation coefficient of 0.990, and the relative standard deviation (RSD) was determined to be 5.8%. The average concentration of $ONOO^-$ from a rat plasma sample (n = 5) was determined to be 4.52 ± 0.33 μM., which is comparable to the values previously reported.[19,35−38] The $ONOO^-$ concentration recovery was between 95% and 98%, which clearly indicates the potentiality of this $ONOO^-$ sensor for detection in real biological samples.

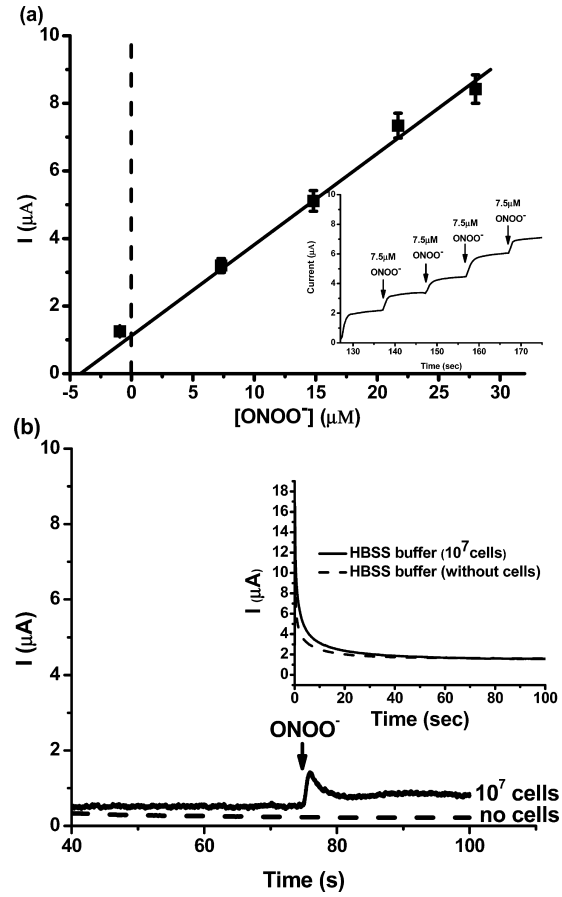

Figure 5. (a) Amperometric responses (inset) and a standard addition plot (main) obtained in spiked rat plasma samples. (b) Chronoamperogram illustrating the variation of $ONOO^-$ concentration with time when transferred from cell-free HBSS to HBSS containing 10^7 YPEN-1 cells. (b, inset) Chronoamperograms showing different $ONOO^-$ concentrations with time in cell-free HBSS (dashed line) and HBSS containing 10^7 YPEN-1 cells (solid line).

Cell Culture Sample Analysis. In addition to blood plasma experiments, the $ONOO^-$ microbiosensor was also used to probe the concentration change of $ONOO^-$ in cultured cells. Figure 5b shows the extracellular signals of rat glioma YPEN-1 cells. The present studies showed that $ONOO^-$ production by phorbol myristate acetate (PMA)-stimulated cells was induced by oxidative stress. When the $ONOO^-$ microbiosensor was removed from the PBS buffer without cells and placed into the Hank buffer saline solution (HBSS) containing stimulated cells, a basal level of $ONOO^-$ was detected with the chronoamperometric technique. A current response of 1.2 μA corresponding to 8.0 (±0.5) $\times 10^{-8}$ M $ONOO^-$ was elucidated. These data demonstrated that PMA induced cells to secrete $ONOO^-$. Thus, the direct in vitro monitoring of cells for $ONOO^-$ related to oxidative stress will be a useful system for biosensor applications such as drug screening.

CONCLUSIONS

A peroxynitrite microbiosensor based on manganese ion (Mn^{2+}) complexed onto the nanostructured conducting polymer (pDPB) was fabricated for the measurement of spiked peroxynitrite in rat plasma sample as well as for the

(36) Tsukahara, H.; Ishida, T.; Mayumi, M. *Nitric Oxide* **1999**, *3*, 191–198.
(37) Lim, C. H.; Dedon, P. C.; Deen, W. M. *Chem. Res. Toxicol.* **2008**, *21*, 2134–2147.
(38) Amatore, C.; Arbault, S.; Guille, M.; Lemaitre, F. *Chem. Rev.* **2008**, *108*, 2585–2621.

in vitro peroxynitrite detection stimulated by PMA in cultured cells. The present microbiosensor exhibited a wide linear range between 2.0×10^{-8} and 5.0×10^{-7} M with a detection limit of 1.9 ($\pm$0.2) $\times 10^{-9}$ M. The microbiosensor was calibrated for experiments. The biosensor surface can be easily regenerated. The response time of this microbiosensor was within 15 s; thus, it can be used to monitor the extracellular fluctuation of peroxynitrite in biological samples. The spiked peroxynitrite concentrations were determined in rat blood plasma. PMA stimulated cells to release peroxynitrite during oxidative stress. Thus, the peroxynitrite biosensor could be an effective tool for monitoring changes in in vitro extracellular peroxynitrite levels in response to stimulant drug exposure.

ACKNOWLEDGMENT

This research was supported by the Midcareer Researcher Program through an NRF grant funded by the MEST, S. Korea (Grant No. 20100029128).

Received for review August 1, 2010. Accepted November 5, 2010.

AC102041U